Efficient loading of a magnetic waveguide on an atom chip

Peter D. D. Schwindt,* Eric A. Cornell, Tetsuo Kishimoto,† Ying-Ju Wang, and Dana Z. Anderson
Department of Physics, University of Colorado, and JILA, National Institute of Standards and Technology and University of Colorado, Boulder, Colorado 80309-0440, USA

(Received 15 October 2004; revised manuscript received 11 April 2005; published 18 August 2005)

We demonstrate efficient loading of neutral atoms into a magnetic waveguide produced by the magnetic fields of microfabricated current-carrying conductors. The lithographically patterned conductors on this "atom chip" can be used to make a variety of guiding and trapping structures for manipulating cold atoms and Bose-Einstein condensates. A three-chamber vacuum apparatus collects atoms in a magneto-optical trap, precools them via evaporative cooling, and delivers them to the final chamber containing the atom chip. We describe in detail how the precooled atomic cloud is transferred from a macroscopic magnetic Ioffe-Pritchard trap to the microscopic magnetic waveguide on the atom chip 21 cm away. Permanent magnets provide a confining two-dimensional quadrupole field to guide the atoms between the two chambers while longitudinally the cloud is allowed to freely expand during the transfer. Strategically placed coils are used to control the longitudinal size and speed of the atomic cloud as it is loaded on the atom chip.

DOI: 10.1103/PhysRevA.72.023612 PACS number(s): 03.75.Be, 03.75.Nt, 32.60.+i, 32.80.Pj

I. INTRODUCTION

Efforts to integrate atom optical elements onto a small substrate seek to miniaturize atom optical devices and possibly achieve a level of system complexity that would be difficult with free-space configurations. An integrated "atom chip" contains microfabricated elements placed on a substrate that can manipulate atoms on micron length scales. Atom chips using micro-optical elements [1] and patterned magnetic materials [2,3] have been demonstrated. However, most chip-based experiments to date use lithographically patterned conductors to produce magnetic fields for guiding and trapping. On-chip magnetic waveguide experiments with cold atoms have demonstrated a series of guiding techniques [4–6], beamsplitters [7,8], and switches [9]. Atoms can also be confined on-chip in magnetic microtraps [6,10] and even be transported with an atom motor [11].

Atomic coherence is a prerequisite for certain atom optics applications, such as atom waveguide interferometers [12–15] and quantum information processing [16,17]. As coherent atomic sources, Bose-Einstein condensates (BEC's) go hand-in-hand with much of the atom-chip work. BEC's are produced in three different scenarios. The scenarios are distinguished firstly by whether the magneto-optic trap (MOT) is located in proximity to the chip or not, that is, whether or not the chip and the MOT are subject to the same background pressure. They are distinguished secondly by whether the BEC formation is done off-chip or on-chip. With the chip's surface only a few microns to a few hundred microns away from the atoms, an on-chip magnetic microtrap is not easily loaded by a standard (MOT), which traditionally sits in free space, centimeters away from any surfaces. Several research groups have employed a mirror MOT where a reflective coating is deposited on the surface of the atom chip to produce the light fields for laser cooling and trapping such that the MOT is loaded millimeters away from the surface [3,6,10]. Once in the mirror MOT, the atoms are transferred into the microtrap and cooled via radio frequency evaporation to form a BEC [18–21]. In such experiments the pressure is temporally modulated, first to be high in order to capture a large number of atoms in the MOT, and then low to support efficient evaporative cooling and achieve long atom coherence times. Another approach utilizes a MOT and BEC production that is far from the atom chip and then transports the BEC to the chip for loading into a microtrap as demonstrated by Ref. [22]. We, as well as the work of Ref. [23], have utilized a MOT that is far from the chip, load the atoms onto it after traversing an evaporative precooling stage, and finally cool the atoms to condensation on the chip.

MOT's that are small and in proximity to the chip are an elegant solution to cold atom sources, one that appeals to the motif of atom chip technology. Typical atom numbers, though, are much smaller than what is commonly achieved with a separated large MOT. Moreover, temporal modulation of the pressure is sometimes unfeasible or undesirable, especially as one considers the possibility of continuous BEC sources [24]. Thus, techniques to transport cold atoms and load them onto a chip are likely to continue playing a role in atom chip technology. This work presents an experimental study of a scheme we have utilized to load ultracold atoms into an atom chip waveguide from a "distant" Ioffe-Pritchard trap used for precooling atoms by forced evaporation.

In our case, loading requires the atoms to be transported from an evaporation chamber containing the Ioffe-Pritchard trap to an application chamber containing the atom chip 21 cm away. For the transport, we launch the sample of atoms from the Ioffe-Pritchard trap into a macroscopic magnetic guide formed by permanent magnets, essentially creating a pulsed beam of atoms. The atoms are allowed to

*Present address: National Institute of Standards and Technology, Boulder, Colorado 80305, USA.

†Present address: PRESTO, Japan Science and Technology Agency(JST), and Department of Applied Physics, School of Engineering, The University of Tokyo, Hongo 7-3-1, Bunkyo-ku, Tokyo 113-8656, Japan.

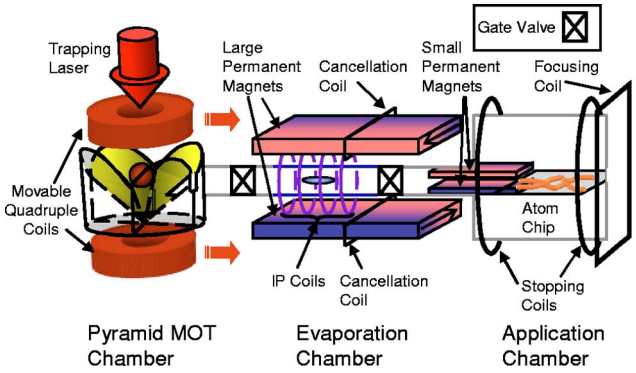

FIG. 1. (Color online) The three-chamber vacuum system. Around the vacuum system are the coils and magnets used to transfer the atoms between the chambers. The gate valves between chambers are open during normal operation and can be closed to allow modification of one chamber without affecting the others. The shading and the arrows on the permanent magnets indicate the direction of magnetization.

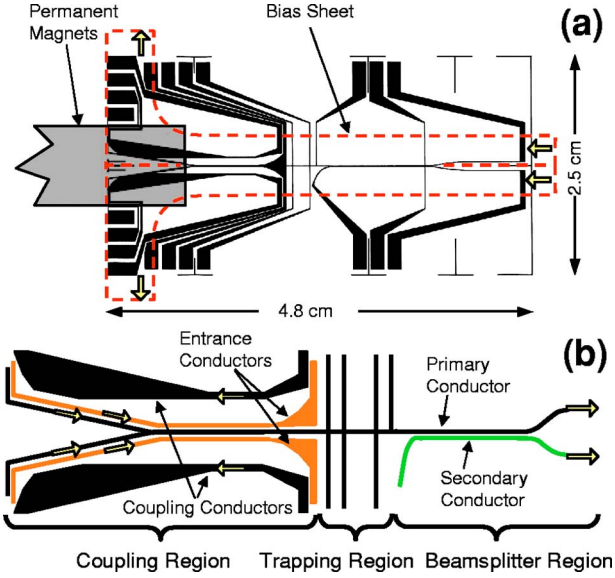

FIG. 2. (Color online) (a) The conductor pattern on the atom chip (to scale). The small permanent magnets overlap the chip by 9 mm. The dotted line shows the outline of the bias sheet that is imbedded in the copper block under the atom chip. It is actually two 3 mm wide conductors lying side-by-side running the length of the chip. The arrows indicate the direction of the current in the bias sheet. (b) The central region of the atom chip is expanded to show the general shape of the wires (not to scale). The atoms move from left to right along the primary conductor.

expand freely in the direction of propagation for a time, after which we use coils to longitudinally focus [25] and decelerate the atoms as they move onto the atom chip. The permanent magnetic guide merges smoothly with the magnetic waveguide on the atom chip so that the atoms are efficiently loaded onto the chip.

II. THE APPARATUS

Our experimental apparatus is a three-chamber vacuum system shown in Fig. 1. The gate valves between each chamber allow us to modify one chamber without affecting the integrity of the vacuum in another. In particular, we can rapidly change out the atom chip (in 3 days) without affecting the other two chambers. In the first chamber of our system, the pyramid MOT chamber, we collect ^{87}Rb atoms from a room temperature rubidium vapor in a pyramid MOT [26] where an inverted pyramidal mirror creates the necessary six beams for the MOT from a single large laser beam. After the pyramid MOT collects 2×10^{10} atoms, the light for the MOT is switched off, and the atoms are optically pumped into the $F=1$ ground state. Then, the current in the movable quadrupole coils is switched on to provide a gradient of 60 G cm^{-1} in the strong direction to magnetically trap 6×10^{9} atoms in the $|F=1,m_F=-1\rangle$ state. We increase the gradient of the quadrupole coils to 175 G cm^{-1} and move the coils on a servo-controlled linear track to transport the trapped atoms to the evaporation chamber and into a hybrid Ioffe-Pritchard trap. The trap is formed by four coils, which axially confine the atoms and provide the quantization bias field, and by two permanent magnets, which radially confine the atoms with a 2-D quadrupole field. The gradient provided by the magnets is 650 G cm^{-1}. Typical radial and axial trap frequencies in our trap are $\omega_\perp=2\pi\times170$ Hz and $\omega_\parallel=2\pi\times7$ Hz, respectively. The lifetime in the evaporation chamber (>100 s) is sufficiently long to allow efficient RF evaporation to cool the atomic sample in the trap, and by setting the depth of the final RF cut, we can control the temperature of the cloud that is sent to the application chamber. In fact, we can cool the cloud to quantum degeneracy and make a BEC containing $\sim2\times10^5$ atoms. More details on the operation of the first two chambers of our system can be found in Refs. [27,28].

The application chamber is a large chamber designed to house the atom chip while giving good optical access along the length of the chip. The atom chip is glued to a machined copper block that also supports the two small permanent magnets and a bias sheet. The bias sheet is a 6×1.6 mm^2 rectangular conductor that runs 1.4 mm under the surface of the atom chip to provide a transverse bias field, B_t [Fig. 2(a)]. This assembly is mounted in the application chamber on a single flange, which also contains 22 electrical feedthroughs to supply current to the atom chip and the bias sheet. Polyimide insulated copper wires lead from the vacuum feedthroughs to the chip where they are attached to the chip's conductors with a silver/tin solder.

III. THE ATOM CHIP

The chip consists of copper conductors formed on an aluminum nitride substrate, using standard lithographic and electroplating techniques [29]. The main guiding wires are 20 μm wide and are electroplated to a thickness of ~10 μm. The atom chip is comprised of three regions: a coupling region, a trapping region, and a beam splitter region [Fig. 2(b)]. Through these three regions runs the primary waveguide conductor that produces the central atom waveguide on the chip. The waveguide is formed by the combined magnetic fields produced by the primary conductor's current and

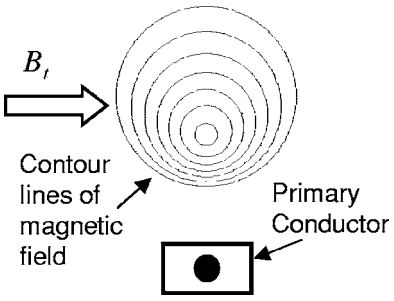

FIG. 3. The "bias-field guide." The transverse bias field, B_t, from the bias sheet cancels the field from the conductor at a distance from the conductor (typically 50–100 μm).

that of the bias sheet, which carries a larger current in the opposite direction. The bias field, B_t, from the bias sheet cancels the primary conductor's field at a distance $d = \mu_o I/2\pi B_t$ from the primary conductor, where μ_o is the permeability of free space and I is the current through primary conductor (Fig. 3). A field parallel to the primary conductor, $B_\parallel$, sets the minimum magnetic field seen by an atom in the waveguide to adjust the transverse waveguide frequency. In the trapping region of the chip, perpendicular conductors intersect the primary conductor. A current through these conductors creates a longitudinal trapping potential by adding a field to $B_\parallel$ [10,29]. In the beam splitter region a secondary waveguide conductor parallels the primary conductor to create two waveguides that can be merged and separated by changing B_t in time. The coupling region contains several other conductors whose function is to smoothly merge the waveguide created by the permanent magnets into the waveguide created by the primary conductor.

IV. TRANSFER TO THE ATOM CHIP

For transferring the atoms from the evaporation chamber to the application chamber, we extend the large permanent magnets for the hybrid Ioffe-Pritchard trap to the application chamber. Where these large permanent magnets end, two smaller permanent magnets inside the application chamber extend to overlap the atom chip. These two sets of magnets confine the atoms radially, making a guide for the atoms as they move to the chip. To push the atoms toward the application chamber, we vary in time the longitudinal confinement. We describe this process in more detail in the next section.

The transition from the guide formed by the small permanent magnets to the chip's primary waveguide is designed such that the atoms are able to follow a single magnetic minimum from the magnets into the waveguide. As the atoms move away from the small permanent magnets, the 1600 G cm^{-1} gradient from the magnets decays to zero over a distance of approximately 1 cm. Typically, the bias sheet carries 30 A to provide a transverse bias field of 23 G; the current exits the bias sheet symmetrically out both sides of the T at the beginning of chip to avoid "bumps" in the longitudinal magnetic field that would be produced by an asymmetric design. Thus, the transverse bias field increases as the

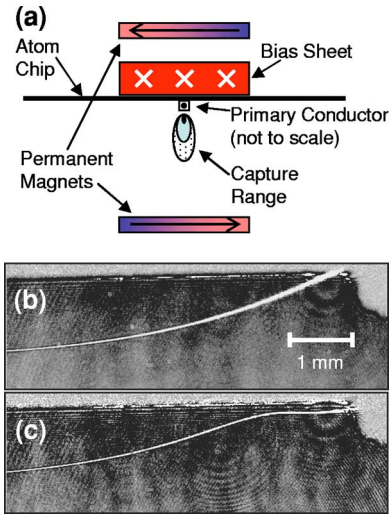

FIG. 4. (Color online) (a) The cross section of the atom chip assembly (to scale). The capture range of the primary waveguide is depicted for three conditions by the ellipses. The conditions are $I_{primary}$=0.5 A (smallest), $I_{primary}=I_{entrance}$=0.5 A (middle), and $I_{primary}=I_{entrance}$=0.5 A, $I_{coupling}$=5 A (largest). See Fig. 2(b) for the wire configuration in the coupling region. (b) This image shows the transverse bias field (B_t=23 G) bringing the atoms up to the chip. None of the wires in the coupling region are on so the atoms crash into the chip. The atoms are moving from left to right. (c) In this image $I_{primary}=I_{entrance}$=0.5 A and $I_{coupling}$=5 A. The atoms are captured in the waveguide.

atoms move past the T of the bias sheet and remains nearly constant along the rest of the atom chip. The quadrupole field of the magnets and the transverse bias field are oriented such that as the atoms move out of the small permanent magnets' weakening field, the transverse bias field deflects the magnetic minimum of the magnets up toward the surface of the chip. Figure 4(b) shows the atoms following the guide formed by the fields from the magnets and the bias sheet up to the chip's surface. With the permanent magnets and the atom chip aligned properly, the magnetic minimum is directed toward the primary guiding conductor, and the primary conductor "captures" the magnetic minimum of permanent magnets at a certain point along the chip, causing the atoms to be coupled into the waveguide. The atoms are seen to move into the primary waveguide in Fig. 4(c). The atoms are typically guided 50–100 μm below the primary conductor.

If the atom chip and the permanent magnets are not well aligned, the primary wire will not capture the atoms, and the atoms will crash into the substrate. By modeling the fields produced by the magnets and the conductors of the atom chip and bias sheet (see the Appendix), we can calculate the radial position, depth, and radial frequency of the magnetic guide as a function of longitudinal position. By simulating a misalignment between the permanent magnets and the atom chip, we can determine a capture range for the primary conductor, that is, an alignment tolerance such that the atoms will be coupled into the primary waveguide. For a primary conductor current of 0.5 A and B_t=20 G, the horizontal capture range of the waveguide is ±0.05 mm. The magnetic

minimum from the magnets must be offset below the primary conductor, making the vertical capture range 0.5–0.8 mm below the chip [Fig. 4(a)]. The copper block that supports the chip and the magnets aligns the two relative to each other to a tolerance of ±0.05 mm, though we are uncertain how well the magnetic minimum of the permanent magnets is aligned to the geometric center of the magnets.

To increase the capture range of the chip's waveguide, we utilize additional conductors in the coupling region [Fig. 2(b)]. The "entrance" conductors run close to the primary conductors, separated by 40 μm (center-to-center). With a 0.5 A current running in the same direction as the primary conductor, the entrance wires add to the field created by the primary conductor, increasing the capture range to ±0.25 mm in the horizontal direction and to 0.5–1.6 mm in the vertical direction. The "coupling" conductors carry a current of 5 A each in the opposite direction of the primary conductor current and act to repel the minimum from the permanent magnets, pushing it toward the primary conductor. The coupling conductors are spaced 1 mm away from the primary conductor, and their width at the narrowest point is 0.1 mm. By using all of the conductors in the coupling region, the capture range is ±0.5 mm in the horizontal direction, and 0.5–2.0 mm in the vertical direction. The model of the fields shows that the optimal loading, i.e., highest depth and radial frequency of the guide, occurs with no horizontal offset and a vertical offset of 1.15 mm.

The conductors in the coupling region start widely separated and taper in symmetrically over a length of a 1–1.3 cm. This geometry addresses a number of issues. We apply $B_{\|}=3$ G to set the magnetic field at the bottom of the guide. Currents that flow perpendicular to $B_{\|}$ produce fields that add to $B_{\|}$ and create barriers in the longitudinal potential that can reflect the atoms or dips in the potential that could cancel $B_{\|}$, giving rise to Majorana spin flips. To avoid this problem, we bring in the currents symmetrically at the beginning of the chip. The fields from these opposite currents cancel along the symmetry axis of the primary conductor. This solves the problem provided the atoms are perfectly centered over the chip, but the guide may be offset horizontally due to a misalignment of the permanent magnets. The larger the horizontal offset, the larger the longitudinal field from the perpendicular currents becomes at the guide center. For this reason, in the first section of the chip, the conductors are tapered to minimize the longitudinal field from the currents. The maximum longitudinal field from the coupling region and the T in the bias sheet is calculated to be 0.8 G on the edge of the horizontal capture range—sufficiently small for our typical center of mass speeds of 10–30 cm s^{-1}.

V. LONGITUDINAL CONTROL OF THE TRAVELING ATOMIC CLOUD

Atoms are moved along the permanent magnetic guide from the evaporation chamber to the atom chip with time-varying fields produced by several external coils (Fig. 1). These coils control the center-of-mass velocity and the longitudinal expansion of the cloud. This control is required for several reasons: The cloud must be halted over the center of an on-chip magnetic trap. The cloud also needs to be focused longitudinally for efficient trap loading. Moreover, the transfer ought to be adiabatic or nearly so. As the atoms move to the chip, there are several points along the guide where the atoms can experience large transverse accelerations if they are moving too quickly. For example, Fig. 4(c) shows an image of the atoms as they are coupled into the primary waveguide, showing a sharp bend in the trajectory of the atoms. In this image the atoms are moving at 35 cm s^{-1}, and the transverse acceleration, $a_{\perp}$, at this sharp bend is approximately 900 cm s^{-2}. The radial frequency of the guide, $\omega_{\perp}$, at the sharpest bend sets a condition on the maximum acceleration atoms can have to move onto the chip adiabatically, $a_{\perp} \ll \omega_{\perp}^2 \sigma_0$ where $\sigma_0 = \sqrt{\hbar/m\omega_{\perp}}$. At the bend $\omega_{\perp} \approx 2\pi \times 500$ Hz giving $\omega_{\perp}^2 \sigma_0 = 475$ cm s^{-2}. Another point where the atoms may experience a transverse acceleration is where the fields from the large and small permanent magnets overlap. A slow velocity maintained during the chip loading minimizes heating. Using the model of the fields in the coupling region to determine the acceleration the atoms experience as they are loaded into the primary waveguide, we find that the velocity should be $\leqslant 10$ cm s^{-1} for adiabatic loading.

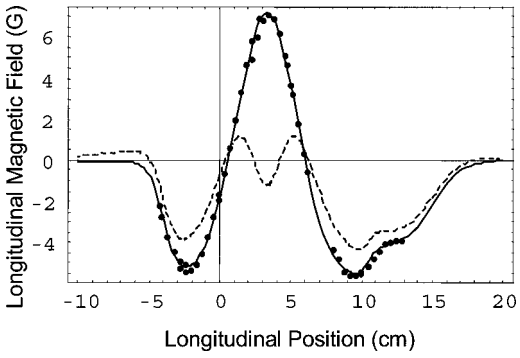

FIG. 5. This plot shows the measured longitudinal field from the large permanent magnets as a function of position measured from the hybrid Ioffe-Pritchard trap center. The atoms chip begins at 20 cm. The solid line is an analytical approximation to the data. The dashed line is the sum of the calculated field of the cancellation coils and the field from the permanent magnets.

In principle the longitudinal degrees of freedom of the cloud are easily controlled by time-varying magnetic fields [25], but maintaining control is made more difficult in our case by imperfections in the permanent magnets. Ideally, the magnets would produce only a radial field having a strong radial gradient. In fact, they produce a spatially changing longitudinal field as well, rather large in magnitude, gradient, and curvature. Figure 5 shows the longitudinal field from our best set of large permanent magnets. The large barrier created by the permanent magnets can be canceled to some extent with a pair of cancellation coils (Fig. 1). With one coil wrapped around each large permanent magnet centered on the position of the magnets' barrier, the cancellation coils reduce the barrier's peak-to-peak amplitude by up to 7 G. The small set of permanent magnets also produces a longitudinal field but, as it is mounted inside the chip chamber, it is inaccessible for field measurements. Measurements of another set of small magnets show a peak-to-peak amplitude of

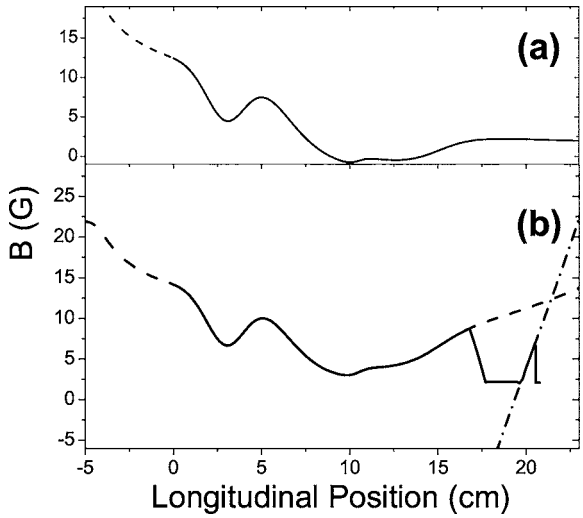

FIG. 6. The longitudinal magnetic field is plotted versus longitudinal position. (a) The plot shows the longitudinal magnetic field and thereby the longitudinal potential the atoms experience from the permanent magnets, the quadrupole coils, and the cancellation coils. (b) The plot shows the total longitudinal field when the focusing coil (dash) and the stopping coils (dot-dash) are used. The solid line shows the field that the center of mass of the cloud experiences at a given longitudinal position. After the center of mass of the cloud reaches 17 cm, the focusing coil has reversed the expansion of the cloud and is ramped off. Then, once the cloud has reached 20 cm the stopping coils are ramped on so that the cloud will be stopped at 21 cm in the trapping region of the chip.

12 G with a stronger gradient than the large magnets because they are more closely spaced. Thus, we have an irregular longitudinal magnetic potential making it difficult to control the speed and the longitudinal spread to the cloud.

We use four sets of coils to accelerate the atoms toward the chip chamber, longitudinally focus the cloud, and stop the cloud at the desired location on the chip. Before the atoms are released from the hybrid Ioffe-Pritchard trap, the servo controlled track positions the moving quadrupole coils −10 cm away from the trap center. Over a period of 100 ms the current of the quadrupole coils is ramped on to provide an accelerating gradient, and the current of the cancellation coils is ramped on to lower the barrier of the large permanent magnets. With these coils active, the Ioffe-Pritchard coils are ramped off over 30 ms so that the atoms find themselves on the potential shown in Fig. 6(a). If no other fields are activated, the atoms arrive at the chip moving at 20 cm s^{-1} after 1 s of travel. Without the cancellation coils we would have to give the atoms much more initial potential energy to overcome the barrier of the permanent magnets. Under these conditions the atoms arrive at the chip moving at 35 cm s^{-1} as is the case in Fig. 4(c).

A current ramp on the focusing coil for a period of 30 ms immediately after the atoms' release controls the longitudinal spreading of the cloud. The atoms propagate along the potential in Fig. 6(b). The focusing coil is a square coil, 30 cm on a side, placed 34 cm away from the hybrid Ioffe-Pritchard trap center. As the cloud propagates away from the trap center, it spreads longitudinally. Once the cloud reaches the minimum of the potential, the front of the cloud is traveling faster than the rear of the cloud, and it has nearly reached its maximum longitudinal extent. Then, as the cloud moves up the potential of the focusing coil, the front of the cloud loses more kinetic energy than the rear, and the rear begins to overtake the front, i.e., the cloud begins to focus longitudinally. The rate at which the cloud focuses is determined by the gradient of the field produced by the coil at the center-of-mass position of the cloud, and the gradient of the coil's potential increases as the atoms move toward the chip. The speed and thus the position at which the atoms come to a focus are determined by the gradient of the focusing coil at the center of the cloud when it is ramped off. In other words, the time at which the focusing coil is switched off controls the focal length of the longitudinal lens. Of course, the focusing coil also reduces the center-of-mass velocity as the cloud moves up its potential.

An additional complication arises when performing a focusing experiment with guided atoms. As the cloud moves through a focus, collisions occur that mix energy between the longitudinal and transverse degrees of freedom. For this reason, we slowly focus the cloud, producing a relative kinetic energy between the front and the back of the cloud that is not significantly greater than the transverse energy of the cloud. We find that in general the faster we focus the cloud, the greater its transverse temperature after focusing. When we first began these focusing experiments, we used small coils (diameter of 3 cm) wrapped around the vacuum chamber between the hybrid Ioffe-Pritchard trap and the atom chip. These small coils proved to have two disadvantages. First, the small size of the coil tends to produce larger gradients focusing the cloud more quickly, and we observed that the transverse temperature can increase by a factor of 4. Second, the small size also causes a large curvature in the field, giving rise to focusing aberrations, and this longitudinal lens would focus only a small portion of the cloud, approximately 20%. We now use the large focusing coil, and we achieve a relatively slow lens while focusing the entire cloud.

To further slow or stop the atoms on the chip, we use two "stopping" coils placed on either side of the chip chamber in an anti-Helmholtz configuration. These coils provide a linear slope with little curvature. As the atoms experience this potential, they are slowed but not focused because on a linear slope every atom's velocity is reduced equally. With the stopping coils we can slow or stop the atoms at almost any location on the chip. Figures 7(b) and 7(c) show a 1.4 μK cloud slowed to 5 cm s^{-1} and <1 cm s^{-1} in the trapping region of the chip. As the cloud slows, the small longitudinal field from current deviations within the primary conductor reveals itself as density variations in the cloud. Figures 7(b) and 7(c) show that the cloud fragments in the area of a T in the main conductor. This occurs because the current expands into the T and thus no longer flows straight down the conductor [22]. We estimate that the T causes a 100 mG feature in the longitudinal field. When there is a cross in the main conductor, the current expands symmetrically, and the effect is minimized. However, careful examination of the stopped cloud shows that there is a small effect, and the atoms bunch up on the "upstream" side of the crosses. Other structure in the cloud is due to small deviations of the average direction

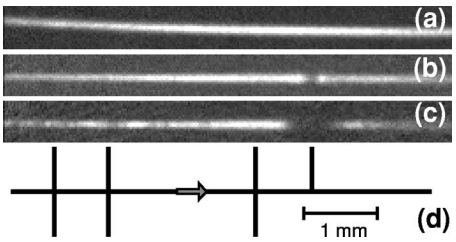

FIG. 7. (a)–(c) The images show a region 6 mm long. Image (a) shows a cloud loaded onto the chip that has been slowed and focused by the focusing coil only and is traveling at 15 cm s^{-1}. It has a temperature of 2.9 μK and a full-width half-maximum longitudinal size of 3 mm. In (b) and (c), the atoms are focused by the focusing coil and slowed by the stopping coils in the trapping region of the chip. Their 1.4 μK temperature is lower because the cloud initially started in the evaporation chamber with a lower temperature. In (b) the cloud is slowed to 5 cm s^{-1} and is split by the T in the primary conductor. In (c) the cloud is slowed to <1 cm s^{-1} and fragmentation occurs from side-to-side deviations of the current in the primary conductor. (d) Schematic of the primary conductor in the trapping region.

of current in the primary conductor as shown by Refs. [22,30].

The transfer between the evaporation chamber and the application chamber delivers the atoms to the chip with near unity efficiency. For example, for a particular set of conditions we measure the atom number in the hybrid Ioffe-Pritchard trap to be $6\pm0.5\times10^5$, and the cloud will have the same atom number on the chip within the measurement error. We have measured unity transfer efficiency for clouds containing up to 2×10^6 atoms, and there is no fundamental limit to the number of atoms that can be efficiently transferred as long as their temperature is less than the depth of the guiding potential. However, the phase space density of the cloud is reduced during the transfer. In the above example when transferring 6×10^5 atoms, the peak phase space density [31] of the cloud is initially 0.2 in Ioffe-Pritchard trap and is reduced to 3×10^{-3} at its minimum longitudinal size on the chip. We believe the loss in phase space density is partially due to the initial longitudinal expansion of the cloud from the hybrid Ioffe-Pritchard trap being not quite adiabatic, but it is largely caused by the imperfect potential produced by the permanent magnets giving rise to transverse accelerations and rapidly changing transverse frequencies. To achieve a BEC in the waveguide, we must deliver a cloud to the chip with a temperature several times greater than the critical temperature, and then we stop and trap the atoms in the trapping region of the chip. With the atoms trapped, we perform radio frequency evaporation to achieve a BEC of 7×10^4 atoms in a microstructure trap on the chip. The details of this result will be reported in a later publication.

VI. CONCLUSION

We have developed a modular three-chamber apparatus for experiments with atoms in microfabricated magnetic waveguides on an atom chip. We use a high-efficiency macroscopic permanent magnetic guide to direct a sample of precooled atoms to the atom chip. Using a time-varying magnetic field with nonzero curvature, we form a lens for the cloud as it moves to the chip such that it comes to a focus on the chip. Using a field with a constant gradient, we can slow or stop the cloud at any location on the chip. The stopped atoms can be loaded into a magnetic microtrap for further cooling to form a BEC. Currently, we are using the BEC as an atomic source to study magnetic waveguide interferometry.

ACKNOWLEDGMENTS

We thank Leslie Czaia for her technical assistance, Victor Bright, Seth Frader-Thompson, and R. A. Saravanan for making the atom chip, and Alex Zozulya for helpful discussions. We gratefully acknowledge the support of the Army Research Office and the Office of the Secretary of Defense through a MURI program in Ultracold Atom Optics Science and Technology (Grant No. DAAD19-00-1-0163), the Office of Naval Research (Grant No. N00014-03-1-0551) and the National Science Foundation (Grant No. PHY-0096822).

APPENDIX: MAGNETIC FIELD MODEL

Our ability to transport the atoms from the evaporation chamber to the application chamber and onto the atom chip is greatly aided by modeling the magnetic fields produced by the various field-producing elements in the experiment. We use analytic approximations to calculate the magnetic field from the various elements. We use the transverse components of the field to estimate the capture range of the atom chip and the adiabaticity of the transfer into the waveguide. The longitudinal field provides the potential that accelerates, decelerates, and focuses the atoms during their transport to the chip. By numerically integrating individual atomic trajectories through the magnetic potential, we estimate the experimental parameters necessary for achieving a well longitudinally focused and stopped cloud at any point on the chip.

The components producing radial fields are the permanent magnets, the bias sheet, and the conductors on the atoms chip. The permanent magnets are modeled as producing a 2-D quadrupole field whose strength varies with the longitudinal distance,

$$\mathbf{B_{Perm}} = B' f(z) \begin{pmatrix} y \\ x \\ 0 \end{pmatrix}, \tag{A1}$$

where B' is the gradient produced by the magnets, the longitudinal decay function is

$$f(z) = \frac{1}{e^{a(z-b)}+1}, \tag{A2}$$

and a and b are parameters that determine the longitudinal decay of the magnets. The functional form of $f(z)$ and the values of B', a, and b are experimentally determined by measuring the transverse gradient of a set of magnets as a function of longitudinal position. We found $B'=650$ G cm^{-1}, $a=0.76$ cm^{-1}, and $b=0.027$ cm for the large permanent mag-

nets and $B'=1600$ G cm^{-1}, $a=4.1$ cm^{-1}, and $b=0.0039$ cm for the small permanent magnets. In $f(z)$, z is measured from one end of the permanent magnets. If in the calculation both ends of the magnets need to be included, $f(l-z)$ is multiplied by $\mathbf{B_{Perm}}$ to simulate the decay of the field at the other end, where the two ends of the magnets are located at $z=0$ and l.

The conductors on the atom chip are all approximated as infinitely thin wire segments. This approximation is sufficiently accurate as long as the distance to the conductor is greater than its width and depth. The field for a segment of wire lying along the z axis with one end at the origin and other at $z=d$ is

$$\mathbf{B_{Wire}} = \frac{\mu_0 I}{4\pi(x^2+y^2)}\left(\frac{z}{\sqrt{x^2+y^2+z^2}} - \frac{z-d}{\sqrt{x^2+y^2+(z-d)^2}}\right) \times \begin{pmatrix} -y \\ x \\ 0 \end{pmatrix}, \tag{A3}$$

where I is the current through the wire and μ_0 is the permeability of free space. To model the conductors on the chip, we simply place wire segments as shown in Fig. 2(b). Where there is a wide flat conductor as is the case for the coupling conductors, we can place several equally spaced segments side by side such that the spacing between wire segments is less than the distance from the conductor to the point of interest (the guide center).

The bias sheet can be modeled in two ways. It can be approximated as an infinitely long, infinitely thin sheet of current where its field is given by

$$\mathbf{B_{Sheet}} = \frac{\mu_0 I}{2\pi w}\begin{pmatrix} \arctan\left(\frac{y}{x-w/2}\right) - \arctan\left(\frac{y}{x+w/2}\right) \\ \frac{1}{2}\ln\left(\frac{(x+w/2)^2+y^2}{(x-w/2)^2+y^2}\right) \\ 0 \end{pmatrix}, \tag{A4}$$

where w is the width of the sheet. Here the sheet is lying in the x-z plane with the current running in the z direction. Although Eq. (A4) does not account for the fact the bias sheet is T shaped at the front to the atom chip, the approximation is sufficient for calculating the capture range of the primary waveguide since the small permanent magnets overlap the bias sheet T by 9 mm, and where the gradient from the magnets is strong, the quadrupole zero is minimally displaced by a transverse field. However, we also need to account for the longitudinal field produced by the T shape in the bias sheet in case the magnets are misaligned and the guide center is not centered over the primary conductor. To calculate this field, we use the infinitely thin wire segments to model the 90° bend in the current. Each conductor of the bias sheet is 3 mm wide [Fig. 2(a)], and we use three parallel segments spaced by 1 mm to model each of the two conductors in the sheet.

Several coils produce the time-varying longitudinal field that transports the atoms. We are mainly interested only in the field along the axis of a coil, which is given by

$$\boldsymbol{B}_{Coil} = \frac{\mu_0 IN}{2}\frac{R^2}{(R^2+z^2)^{3/2}}, \tag{A5}$$

where I is the current through the coil, N is the number of turns, and R is the radius of the coil. The Ioffe-Pritchard coils and the slowing coil are in fact square modifying the formula slightly:

$$\boldsymbol{B}_{Square} = \frac{2\mu_0 IN}{\pi}\frac{R^2}{(R^2+z^2)(2R^2+z^2)^{1/2}}, \tag{A6}$$

where R in this case is half the length of the side of the coil. To model the cancellation coils that are wrapped around the large permanent magnets, we use appropriately placed wire segments following Eq. (A3). The calculated field from the cancellation coils added to the field of the large permanent magnets is shown in Fig. 5. The moving quadrupole coils are used to accelerate the atoms toward the application chamber, and their approximate field along the guide center is

$$\boldsymbol{B}_{Quad} \approx \frac{24\mu_0 IN}{\pi}\frac{R^2 S\{70R^2z^2+[S^2+4(R^2+z^2)]^2\}z}{[S^2+4(R^2+z^2)]^{9/2}}, \tag{A7}$$

where S is the separation of the two coils and z is measured from the geometric center of the coils.

To model the longitudinal dynamics of the cloud as it is transported to the chip, we sum all of the longitudinal fields together and integrate the atomic trajectories as we vary the longitudinal fields in time. The differential equation governing the motion of an individual atom in one dimension is

$$\frac{\mathrm{d}^2 z}{\mathrm{d}t^2} = \frac{-\mu_B g_F m_F}{m_{Rb}}\frac{\partial B_{Total}(z,t)}{\partial z}, \tag{A8}$$

where m_B is the Bohr magneton, g_F is the Lande g-factor, m_F is the magnetic quantum number, m_{Rb} is the mass of the ^{87}Rb, and B_{Total} is the total longitudinal field. To estimate the cloud dynamics, we follow 15 to 20 atomic trajectories. The integration is begun in the Ioffe-Pritchard trap, and each atom is given some initial potential and kinetic energy such that each atom starts with the same total energy equaling the temperature of the cloud. With this model we obtain good qualitative agreement with the experiment, and in cases where the potential is well known, quantitative agreement is achieved. For propagation to the atom chip, the unknown longitudinal magnetic field from the small permanent magnets prevents quantitative agreement with the experiment. Nevertheless, the model aids us greatly in designing the size, the number of turns, and the placement of the coils, although the exact timing of when to turn the coils on and off and the exact current through the coils needs to be determined experimentally.

[1] R. Dumke, T. Muther, M. Volk, W. Ertmer, and G. Birkl, Phys. Rev. Lett. **89**, 220402 (2002).
[2] A. I. Sidorov, R. J. McLean, F. Scharnberg, D. S. Gough, T. J. Davis, B. J. Sexton, G. I. Opat, and P. Hannaford, Acta Phys. Pol. B **33**, 2137 (2002).
[3] M. Vengalattore, W. Rooijakkers, and M. Prentiss, Phys. Rev. A **66**, 053403 (2002).
[4] D. Müller, D. Z. Anderson, R. J. Grow, P. D. D. Schwindt, and E. A. Cornell, Phys. Rev. Lett. **83**, 5194 (1999).
[5] N. H. Dekker, C. S. Lee, V. Lorent, J. H. Thywissen, S. P. Smith, M. Drndić, R. M. Westervelt, and M. Prentiss, Phys. Rev. Lett. **84**, 1124 (2000).
[6] R. Folman, P. Krüger, D. Cassettari, B. Hessmo, T. Maier, and J. Schmiedmayer, Phys. Rev. Lett. **84**, 4749 (2000).
[7] D. Müller, E. A. Cornell, M. Prevedelli, P. D. D. Schwindt, A. Zozulya, and D. Z. Anderson, Opt. Lett. **25**, 1382 (2000).
[8] D. Cassettari, B. Hessmo, R. Folman, T. Maier, and J. Schmiedmayer, Phys. Rev. Lett. **85**, 5483 (2000).
[9] D. Müller, E. A. Cornell, M. Prevedelli, P. D. D. Schwindt, Y.-J. Wang, and D. Z. Anderson, Phys. Rev. A **63**, 041602(R) (2001).
[10] J. Reichel, W. Hänsel, and T. W. Hänsch, Phys. Rev. Lett. **83**, 3398 (1999).
[11] W. Hänsel, J. Reichel, P. Hommelhoff, and T. W. Hänsch, Phys. Rev. Lett. **86**, 608 (2001).
[12] O. Zobay and B. M. Garraway, J. Phys. B **178**, 93 (2000).
[13] E. A. Hinds, C. J. Vale, and M. G. Boshier, Phys. Rev. Lett. **86**, 1462 (2001).
[14] W. Hänsel, J. Reichel, P. Hommelhoff, and T. W. Hänsch, Phys. Rev. A **64**, 063607 (2001).
[15] E. Andersson, T. Calarco, R. Folman, M. Andersson, B. Hessmo, and J. Schmiedmayer, Phys. Rev. Lett. **88**, 100401 (2002).
[16] E. A. Hind and I. G. Hughes, J. Phys. D **32**, R119 (1999).
[17] T. Calarco, E. A. Hinds, D. Jaksch, J. Schmiedmayer, J. I. Cirac, and P. Zoller, Phys. Rev. A **61**, 022304 (2000).
[18] W. Hänsel, P. Hommelhoff, T. W. Hänsch, and J. Reichel, Nature (London) **413**, 498 (2001).
[19] M. P. A. Jones, C. J. Vale, D. Sahagun, B. V. Hall, and E. A. Hinds, Phys. Rev. Lett. **91**, 080401 (2003).
[20] A. Kasper, S. Schneider, Ch. vom Hagen, B. Engeser, T. Schumm, I. Bar-Joseph, R. Folman, L. Feenstra, and J. Schmiedmayer, J. Opt. B: Quantum Semiclassical Opt. **5**, S143 (2003).
[21] Y. J. Lin, I. Teper, C. Chin, and V. Vuletic, Phys. Rev. Lett. **92**, 050404 (2004).
[22] A. E. Leanhardt, A. P. Chikkatur, D. Kielpinski, Y. Shin, T. L. Gustavson, W. Ketterle, and D. E. Pritchard, Phys. Rev. Lett. **89**, 040401 (2002).
[23] H. Ott, J. Fortágh, G. Schlotterbeck, A. Grossmann, and C. Zimmermann, Phys. Rev. Lett. **87**, 230401 (2001).
[24] P. Cren, C. F. Roos, A. Aclan, J. Dalibard, and D. Guéry-Odelin, Eur. Phys. J. D **20**, 107 (2002).
[25] E. Maréchal, S. Guibal, J.-L. Bossennec, R. Barbé, J.-C. Keller, and O. Gorceix, Phys. Rev. A **59**, 4636 (1999).
[26] K. I. Lee, J. A. Kim, H. R. Noh, and W. Jhe, Opt. Lett. **21**, 1177 (1996).
[27] H. J. Lewandowski, D. M. Harber, D. L. Whitaker, and E. A. Cornell, J. Low Temp. Phys. **132**, 309 (2003).
[28] P. D. D. Schwindt, "Magnetic Traps and Guides for Bose-Einstein Condensates on an Atom Chip," Ph.D. thesis, JILA, University of Colorado, 2003.
[29] J. Reichel, W. Hänsel, P. Hommelhoff, and T. W. Hänsch, Appl. Phys. B: Lasers Opt. **72**, 81 (2001).
[30] S. Kraft, A. Günther, H. Ott, D. Wharam, C. Zimmermann, and J. Fortágh, J. Phys. B **35**, L469, (2002).
[31] The peak phase space density is defined as $n\lambda_{dB}^3$ where n is the number density and λ_{dB} is the de Broglie wavelength at the center of the cloud.